

Journal of

[www. biophotonics-journal.org](http://www.biophotonics-journal.org)

BIOPHOTONICS

 WILEY-VCH

REPRINT

LETTER

2-D mapping of skin chromophores in the spectral range 500–700 nm

Dainis Jakovels* and Janis Spigulis

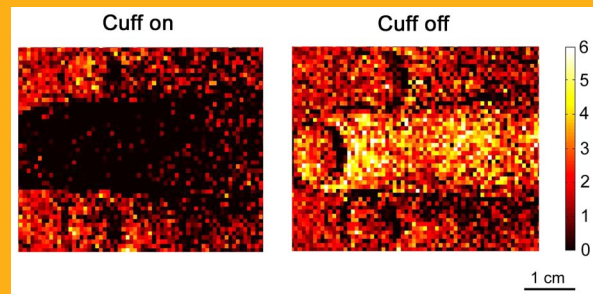
Bio-Optics and Fibre Optics Laboratory, Institute of Atomic Physics and Spectroscopy, University of Latvia, Raina Blvd. 19, LV – 1586, Riga, Latvia

Received 17 August 2009, revised 20 October 2009, accepted 20 October 2009
Published online 9 November 2009

Key words: multi-spectral imaging, haemoglobin, melanin, skin chromophore mapping

PACS: 00.00.Xx, 11.11.Yy

The multi-spectral imaging technique has been used for distant mapping of *in-vivo* skin chromophores by analyzing spectral data at each reflected image pixel and constructing 2-D maps of the relative concentrations of oxy-/deoxy-haemoglobin and melanin. Instead of using a broad visible-NIR spectral range, this study focuses on narrowed spectral band 500–700 nm, speeding-up the signal processing procedure. Regression analysis confirmed that superposition of three Gaussians is optimal analytic approximation for the oxy-haemoglobin absorption tabular spectrum in this spectral band, while superposition of two Gaussians fits well for deoxy-haemoglobin absorption and exponential function – for melanin absorption. The proposed approach was clinically tested for three types of *in-vivo* skin provocations: ultraviolet irradiance, chemical reaction with vinegar essence and finger arterial occlusion. Spectral range 500–700 nm pro-



Relative oxy-hemoglobin concentration maps.

vided better sensitivity to oxy-haemoglobin changes and higher response stability to melanin than two reduced ranges 500–600 nm and 530–620 nm.

1. Introduction

The mapping of *in-vivo* skin chromophores is based on multi-spectral imaging that combines spectral analysis of diffusely reflected light and image analysis, resulting in 2-D maps of the relative concentrations of chromophores, e.g. oxy-/deoxy-haemoglobin and melanin [1, 2]. Such mapping ensures reliable

non-invasive evaluation of skin condition [3–5]. The least-squares regression analysis of a broad visible-NIR spectral range (450–720 nm [2], 460–820 nm [6]) was successfully used to estimate the chromophore content in skin. Drawback of this technique is very time-consuming (proportional to the quantity of spectral information) data acquisition and processing; narrowing of the working spectral range cer-

* Corresponding author: e-mail: dainis.jakovels@gmail.com, Phone: +37 167 225 493, Fax: +37 167 228 249

tainly could speed up the procedure. However, there is a risk to loose specificity and sensitivity to the main skin chromophores, therefore optimal spectral range for skin chromophore mapping should be found [7]. For instance, potential of the reduced spectral range 525–645 nm for imaging of skin haemoglobin oxygen saturation has been demonstrated recently [8]. The third main skin chromophore – melanin – could not be mapped since the measurements were taken for palm skin.

Goal of the present study was to examine spectral interval 500–700 nm and two sub-bands 500–600 nm and 530–620 nm from the point of applicability for simultaneous distant mapping of three main *in-vivo* skin chromophores: oxy-haemoglobin, deoxy-haemoglobin and melanin. Feasibility of this approach was checked by pilot multi-spectral measurements of provoked skin.

2. Experimental

The multi-spectral imaging system *Nuance 2.4* (Cambridge Research & Instrumentation, Inc., USA) and a PC were used for spectral imaging of normal and provoked *in-vivo* skin areas of the forearm. Illumination source was a 100 W tungsten incandescent lamp (intensity fluctuations less than $\pm 2\%$ during the measurement time) with linear polarization filter. This polarizer was oriented orthogonally to the built-in polarizer of *Nuance 2.4*, so significantly reducing the influence of skin specular reflection [9].

The system was adjusted for spatial resolution 0.75×0.75 mm (the pixel size) and spectral resolution 10 nm (bandwidth of the *Nuance 2.4* liquid crystal tuneable filter).

2.1 Data acquisition and processing

The data were collected in an image cube – a stack of intensity images at numerous wavelength bands. Typical time required for creation of the image cube in spectral interval 500–700 nm was ~ 10 s.

The back reflected light intensity (I) values at each pixel were transformed to the optical density (OD) as follows:

$$OD = -\log_{10} \left(\frac{I}{I_0} \right), \quad (1)$$

where I_0 – reflection intensity from the white reference – bended white office paper sheet (spectral reflectance 0.90 ± 0.04 within the 500–700 nm band), attached to the forearm skin. Optical density of the

superficial skin layer has been predicted in frame of the three chromophore absorption model:

$$OD_{\text{predicted}} = a_{\text{OH}} \cdot \varepsilon_{\text{OH}} + a_{\text{DOH}} \cdot \varepsilon_{\text{DOH}} + a_{\text{Mel}} \cdot \varepsilon_{\text{Mel}} + a_{\text{Offset}}, \quad (2)$$

where ε_{OH} , ε_{DOH} and ε_{Mel} denote reference absorption spectra for oxy-hemoglobin (OH), deoxy-hemoglobin (DOH) and eumelanin as melanin (Mel), respectively. a_{OH} , a_{DOH} and a_{Mel} represent the relative chromophore concentration values; a_{Offset} is the difference between the predicted and measured spectra.

The predicted OD spectrum at each image pixel was compared to the measured OD spectrum by solving the nonlinear least-squares problem using the Trust-Region algorithm [10], with subsequent extraction of the corresponding relative concentrations of the skin chromophores [2]. The reference absorption spectra of the three chromophores were taken from the literature data [11, 12].

Analysis of the reference spectra allowed proposing handy analytic expressions that approximated well the tabular data within the spectral interval 500–700 nm. Superposition of three Gaussians proved to be optimal for approximation of the OH spectrum, while superposition of two Gaussians suited well for approximation of the DOH spectrum (Figure 1). The values of multiple determination

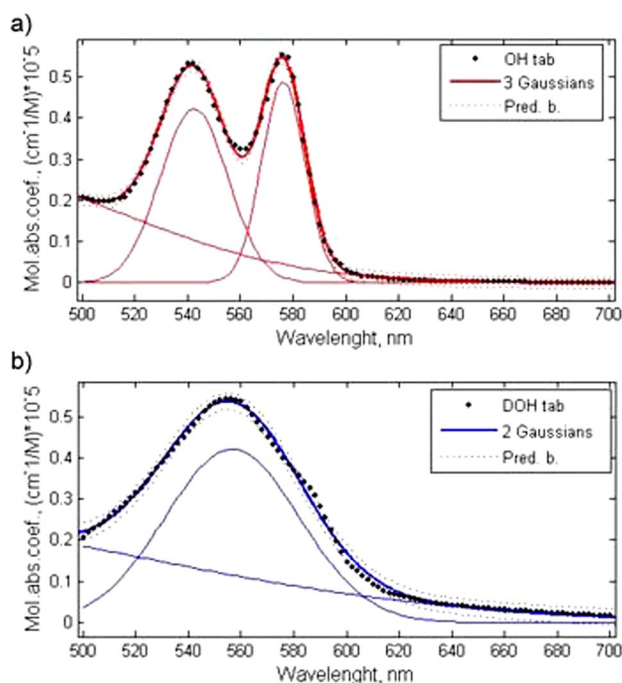


Figure 1 (online color at: www.biophotonics-journal.org) Analytical approximations of the tabular spectra of haemoglobin [12] in the 500–700 nm range: (a) superposition of three Gaussians related to the OH spectrum, (b) superposition of two Gaussians related to the DOH spectrum.

coefficients R^2 were obtained as $R^2_{\text{OH}} = 0.9988$ for oxy-haemoglobin and $R^2_{\text{DOH}} = 0.9973$ for deoxy-haemoglobin. Generally, the Gaussian superposition can be expressed as:

$$f(x) = a_1 \cdot e^{\left(\frac{x-b_1}{c_1}\right)} + a_2 \cdot e^{\left(\frac{x-b_2}{c_2}\right)} + a_n \cdot e^{\left(\frac{x-b_n}{c_n}\right)}, \quad (3)$$

where a , b , c – analytically expressed coefficients and x – wavelength.

Regarding the melanin absorption spectrum, it could be well approximated ($R^2_{\text{Mel}} = 0.9975$) by the exponential function:

$$f(x) = a \cdot e^{-b \cdot x}, \quad (4)$$

where a , b – positive coefficients.

As the next step, the relative values of the respective skin chromophore concentrations a_{OH} , a_{DOH} , a_{Mel} have been determined in *MatLab* at each image pixel, and the chromophore maps representing the planar distribution of the particular chromophore have been constructed. The color scale (Fig-

ures 2, 3) represent the obtained chromophore concentrations relatively to their mean values of the surrounding normal (unprovoked) skin.

2.2 Skin provocations

Three different provocations of skin photo-type 3 (single volunteer) were applied in order to obtain pilot results for the proposed method.

Electrodeless high-frequency discharge Mercury lamp with specific UV-C peak at 253.7 nm was used to irradiate the forearm skin through a mask with 1×1 cm apertures for local irritation. Four different doses (1, 2, 3 and 4 minutes provocation time) were applied to achieve different skin responses. Erythema appeared at all provocation areas in-between 0.5 hours, and skin colour changed from dark red to dark brown in the next days. Five measurement series were taken during the first day – 10, 30, 60, 120 and 240 minutes after the provocation, and the measurements were repeated 1, 2, 3, 4, 7 and 10 days after the provocation.

Vinegar essence was used for chemical skin provocation. Two stripes (7 mm width) were applied for 3 and 5 minutes to achieve different forearm skin reaction intensities. Skin erythema appeared in few minutes. Measurement series were taken 10, 30, 60 and 90 minutes after the provocation.

Finally, a resin cuff for arterial occlusion ($p \sim 150$ mm Hg) was used to reduce skin blood oxygenation in a finger [13]. Measurements were taken during full occlusion and immediately after removal of the cuff.

After appropriate signal processing, the maps of relative chromophore concentrations were created to follow-up the provoked skin responses.

3. Results and discussion

3.1 Comparison of spectral ranges

The spectral range 500–700 nm clearly showed better sensitivity to the OH content changes and higher stability to melanin if compared to the narrower bands 500–600 nm and 530–620 nm. Sensitivity to the OH content changes was evaluated as contrast between provoked area and normal skin, and for the range 500–700 nm it was for $\sim 20\%$ higher than that for both reduced spectral ranges. Stability to melanin was verified by analysing the chemical and mechanical provocations where its concentration increase was not expected; haemoglobin changes in these tests could influence results causing melanin artefacts.

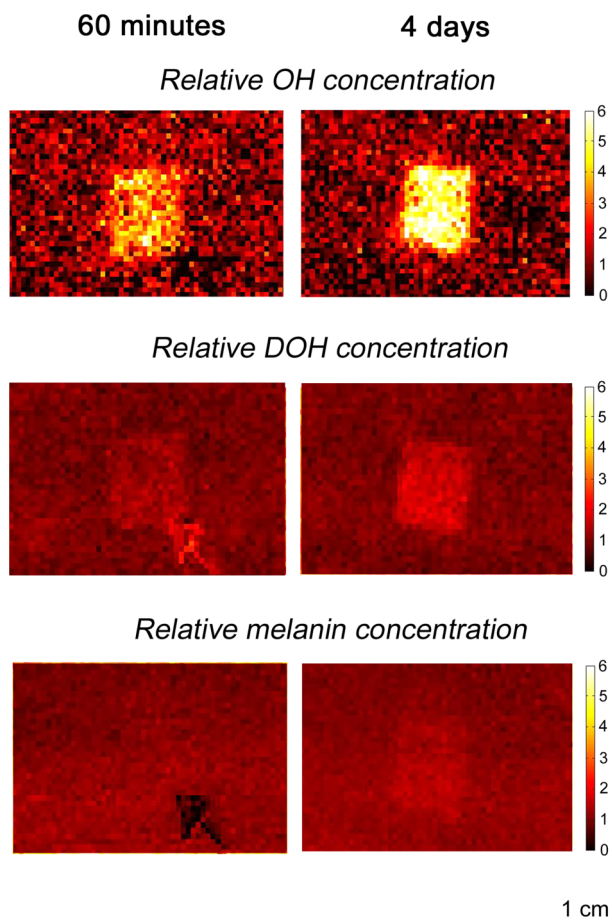


Figure 2 (online color at: www.biophotonics-journal.org) Parameter maps for 4 minutes UV-C provocation 30 minutes (left) and 4 days (right) after irritation. The arrow at the DOH and melanin maps is a pen marker.

False-increased melanin content at the chemical provocation areas was obtained using the narrower spectral ranges 500–600 nm (up to 20%) and 530–620 nm (up to 30%). Consequently, the spectral interval 500–700 nm was chosen as the best option for simultaneous mapping of the three skin chromophores.

3.2 UV-provocation responses

Visible skin erythema appeared within 30 minutes to 2 hours at all UV-provoked areas where increased concentrations of OH (up to 300% compared to normal skin) and DOH (up to 50%) were obtained. Response depended on the provocation doses – higher parameter changes at longer irradiation times were observed. The obtained OH concentration growth was faster than that of the DOH concentration; it reached maximum values (from +300% for 1 min. dose to +400% for 4 min.) within the first day after provocation. High increase of the OH and DOH concentrations (up to +400%) remained for the next 4 days. Later the concentrations gradually returned to the normal level. Slower increase of the parameter values was observed for DOH, but it remained high (from +20% for 1 min. dose to +100% for 4 min.) for a week. Increased melanin concentration appeared on the second day (+5%) after UV-provocation. Higher parameter increase was observed for higher provocation doses (from +5% for 1 min. dose to +20% for 4 min.). In its terms, the results corresponded with previous UV-provocation studies [14].

For illustration, skin chromophore maps related to the UV-provocation (4 minutes) are presented at Figure 2.

3.3 Chemical provocation responses

Visible skin erythema appeared within several minutes after the chemical provocation. Increased OH concentration at the irritated area has been obtained, with maximum ~30 minutes after provocation (+200% for 3 min. dose, +300% for 5 min. dose); more pronounced response corresponded to longer irritation time. Slight increase of DOH concentration (less than 15%) at the chemically provoked area was obtained, as well.

3.4 Responses during and after the finger occlusion

Before occlusion the middle finger maps looked like these for the neighbour fingers. Decreased OH con-

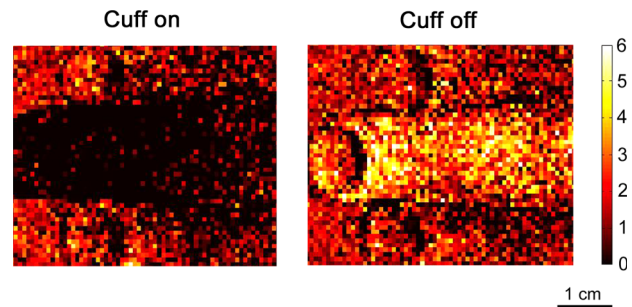


Figure 3 (online color at: www.biophotonics-journal.org) Relative OH concentration maps after the finger occlusion (Cuff on) and immediately after release (Cuff off).

centration (down to 10%) 5 minutes after the arterial finger occlusion was obtained (Figure 3). Right after the cuff release it increased up to 400% relatively to the level before occlusion. Thus the expected OH decrease and overshoot was observed [13]. Slight decrease of DOH (~20%) was obtained during the occlusion. The background was a wooden table with reflectance spectrum similar to the skin spectrum (correlation coefficient 0,86), therefore also the background part of images was processed. However, the intensity distribution of background was about the same at both images (signal standard deviation over all pixels did not differ), which confirms adequate processing.

4. Conclusions

In frame of the simplified 3-chromophore model, the spectral range 500–700 nm is considered to be optimal for simultaneous mapping of OH, DOH and melanin; narrowing of this range (500–600 nm, 530–620 nm) has lead to unacceptable results.

Tabulated molar absorption spectral data for this region can be well approximated by superposition of three Gaussians for OH, superposition of two Gaussians for DOH and exponential function for melanin. Such analytical approximations considerably reduced the signal processing time.

Efficiency of the proposed model and methodology was confirmed by the test measurements. Three different provocations (UV, chemical and arterial occlusion) resulted in notable changes of the skin chromophore content and were well reflected in the obtained maps of the three main chromophores.

The accuracy of chromophore mapping can be further improved taking into account more specific aspects like different light penetration depths at various wavelengths [15] and the scattering effects in skin [16]. Experimental comparison with other skin mapping methods [17] would be performed. There is still poten-

tial to speed-up the mapping procedure by modifying the data processing algorithms. Only pilot results have been reported here; essentially more experimental data are needed for approbation of the new method.

References

- [1] G. N. Stamatias and N. Kollias, In Vivo documentation of cutaneous inflammation using spectral imaging. *J. Biomed. Opt.* **12**(5), 051603 (2007).
- [2] M. A. Ilias, E. Haggblad, and C. Anderson, Visible, hyperspectral imaging evaluating the cutaneous response to ultraviolet radioation. *Proc. SPIE*, Vol. 6441, 644103 (2007).
- [3] L. L. Randeberg, A. M. Winnem, and N. E. Langlois, Skin (Los. Angeles) changes following minor trauma. *Laser Surg. Med.* **39**(5), 403–413 (2007).
- [4] C. Balas, G. Themelis, and A. Papadakis, A Novel Spectral Imaging System: Application on in-vivo Detection and Grading of Cervical Precancers and of Pigmented Skin Lesions. In *Proc. of "Computer Vision Beyond the Visible Spectrum" CVBVS'01 Workshop*, Hawaii, USA, Dec. (2001).
- [5] A. Vogel, V. V. Chernomordik, and S. G. Demos, Using noninvasive multispectral imaging to quantitatively assess tissue vasculature. *J. Biomed. Opt.* **12**(5), 051604 (2007).
- [6] G. Zonios, J. Bykowski, and N. Kollias, Skin, melanin, haemoglobin, and light scattering properties can be quantitatively assessed in vivo using diffuse reflectance spectroscopy. *J. Invest. Dermatol.* **117**(6), 1452–1457 (2001).
- [7] M. E. Eames, J. Wang, and B. W. Pogue, Wavelength band optimization in spectral near-infrared optical tomography improves accuracy while reducing data acquisition and computational burden. *J. Biomed. Opt.* **13**(5), 054037 (2008).
- [8] K. J. Zuzak, M. T. Gladwin, and R. O. Cannon III, Imaging haemoglobin oxygen saturation in sickle cell disease patients using noninvasive visible reflectance hyperspectral techniques: effects of nitric oxide. *Am J. Physiol. Heart. Circ. Physiol.* **285**, H1183–H1189, 2003.
- [9] S. G. Demos and R. R. Alfano, Optical polarization imaging. *App. Opt.* **36**(1), 150–155 (1997).
- [10] R. H. Byrd, R. B. Schnabel, and G. A. Schultz, A trust region algorithm for nonlinearly constrained optimization. *SIAM J. Numer. Anal.*, **24**, 1152–1170 (1987).
- [11] S. Prahl, Tabulated Molar Extinction Coefficient for Hemoglobin in Water, <http://omlc.ogi.edu/spectra/hemoglobin/summary.html>, Last access: August, 2009.
- [12] S. L. Jacques, Extinction coefficient of melanin, <http://omlc.ogi.edu/spectra/melanin/eumelanin.html>, Last access: August, 2009.
- [13] D. J. Clark, T. J. H. Essex, and B. Cater, Skin (Los. Angeles) oxygen saturation imager. *Adv. Exp. Med. Biol.* **428**, 573–577 (1997).
- [14] P. M. Farr, J. E. Besag, and B. L. Diffey, The time course of UVB and UVC erythema. *J. Invest. Dermatol.* **91**(5), 454–457 (1988).
- [15] S. R. Arridge, M. Hiroaka, and M. Schweiger, Statistical basis for the determination of optical pathlength in tissue. *Phys. Med. Biol.* **40**(9), 1539–1558 (1995).
- [16] I. A. Kiseleva and Y. P. Sinichkin, The apparent optical density of the scattering medium: influence of scattering, *Proc. SPIE*, Vol. 4707, 223–227 (2002).
- [17] L. E. Dolotov, I. A. Kiseleva, and Y. P. Sinichkin, Digital imaging of human skin. *Proc. SPIE*, Vol. 5067, 139–147 (2003).